Comparison of Two-Dimensional and Three-Dimensional Carbon Electrode Geometries Affecting Bidirectional Electroosmotic Pumping

Matías Vázquez-Piñón
Tecnologico de Monterrey,
Escuela de Ingeniería y Ciencias,
Ave. Eugenio Garza Sada 2501,
Monterrey, NL 64849, México

Hyundoo Hwang
BBB, Inc.,
26 Samseong-ro 85-gil, Gangnam-gu,
Seoul 06194, South Korea

Marc J. Madou
Department of Mechanical and Aerospace Engineering,
University of California, Irvine
4200 Engineering Gateway,
Irvine, CA 92697-3975

Lawrence Kulinsky[1]
Department of Mechanical and Aerospace Engineering,
University of California, Irvine
4200 Engineering Gateway,
Irvine, CA 92697-3975
e-mail: lkulinsk@uci.edu

Sergio O. Martínez-Chapa[1]
Tecnologico de Monterrey,
Escuela de Ingeniería y Ciencias,
Ave. Eugenio Garza Sada 2501,
Monterrey, NL 64849, México
e-mail: smart@itesm.mx

This study compares fluid velocity magnitude and direction for three different glassy carbon (GC) electrode systems effecting alternating current (AC) electroosmotic pumping. The flow behavior is analyzed for electroosmotic pumping performed with asymmetric coplanar electrodes. Subsequently, effects of adding microposts array of two different heights (40 μm and 80 μm) are studied. Experimental results demonstrate that as peak-to-peak voltage is increased above 10 V peak-to-peak, the flow reversal is achieved for planar electrodes. Utilization of microposts-enhanced asymmetric electrodes blocks the flow reversal and alters the magnitude of the fluid velocity at the application of larger voltages (above 10 V peak-to-peak). Understanding of the consequences of three-dimensional geometry of asymmetric electrodes would allow designing the electrode system for AC electroosmotic pumping and mixing, as well as bidirectional fluid driving with equal forward and backward flow velocities.
[DOI: 10.1115/1.4044266]

Keywords: AC electroosmosis, microfluidics, pumping, high-aspect-ratio electrodes, glassy carbon

[1]Corresponding authors.

Contributed by the Manufacturing Engineering Division of ASME for publication in the Journal of Micro- and Nano-Manufacturing. Manuscript received November 8, 2018; final manuscript received July 8, 2019; published online July 31, 2019. Assoc. Editor: Irene Fassi.

1 Introduction

The carbon-micro-electromechanical systems (MEMS) fabrication process, consisting of photolithographic patterning followed by pyrolysis [1], allows for straightforward and cost-effective pathway for creation of high-aspect-ratio (HAR) glassy carbon (GC) micro-electrodes. GC electrodes have been demonstrated to work well for electrokinetic applications, including dielectrophoretic separations [2] and alternating current (AC) electroosmotic pumping [3]. AC electroosmotic pumping, where planar electrode system is typically utilized [4–6], can be enhanced by employing three-dimensional structures to explore the effect of high-surface-area electrodes on the velocity and direction of the fluid flow.

In AC electroosmosis, a low-amplitude AC potential is applied across two adjacent electrodes to generate an electric field across the fluid. As a result, an induced electric double layer (EDL) is created at the electrodes' surface, formed by the polarized electrode surface and free counter-ions located in the proximity to the electrodes [7], as shown in Fig. 1.

The high-magnitude electric field near the gap between the adjacent electrodes acts on the suspended charges near the electrode surface. This force generates vortices above the electrodes, and the sizes of these vortices depend on the width of the electrodes. The larger vortex is formed over the wider electrode. When wider and more narrow electrodes are placed next to each other, the wider electrode will dominate the overall flow direction, propelling the bulk fluid in the same direction as its vortex, and generating an overall fluid flow going from the narrow electrode, toward the wide electrode, as shown in Fig. 2(*a*).

In this work, we fabricated interdigitated electrode arrays (IDEA) employing the C-MEMS process to explore the effect of high-surface-area electrodes on the AC electroosmotic pumping efficiency in contrast to the widely used planar electrodes. We set an asymmetry ratio for the asymmetric coplanar IDEA of narrow electrode-to-wide electrode (E_N:E_W) to 20:80 μm (see Fig. 2(*a*)). The fabrication sequence involved photolithographically patterned photoresist (PR) to define the planar electrodes, followed by the second PR deposition and patterning to develop microposts atop of the planar structures. Microposts were developed along the electrodes' width, as shown in Fig. 2(*b*). Finally, the structures were pyrolyzed to obtain a monolithic high-surface-area IDEA. Three types of electroosmotic pumps were developed: the pump (*i*) incorporates only the asymmetric coplanar GC electrodes, but in pumps (*ii*) and (*iii*), 40 μm-height and 80 μm-height GC microposts, respectively, were integrated into the micro-electrode systems.

2 Materials and Methods

2.1 Micro-Electrode Fabrication Process. The devices were fabricated following the C-MEMS process, comprising

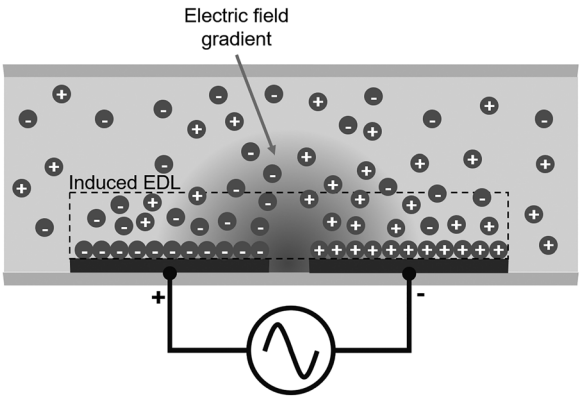

Fig. 1 Induced EDL formation at the electrode surface as an effect of the applied electric field

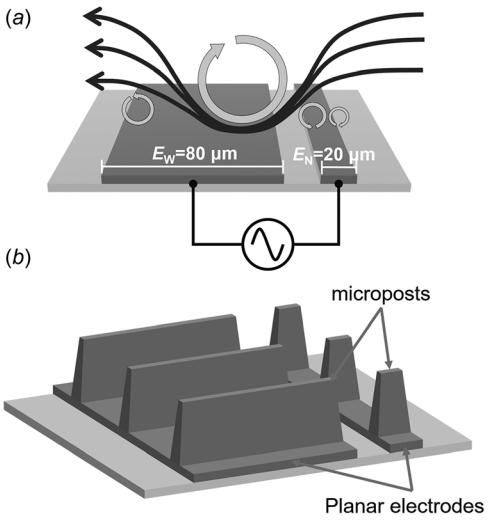

Fig. 2 (*a*) Vortex formation above asymmetric coplanar electrodes by the action of the induced EDL and (*b*) microposts developed on top of the planar electrodes to increase electrode surface area

photolithographic patterning of an organic carbon precursor, followed by pyrolysis in an oxygen free environment. This process was carried out in a class 1000 cleanroom at 22 °C and 38% relative humidity. As a substrate for the carbon structures, 4-in. silicon wafers with a 500 nm thermally grown SiO_2 layer were used. Before processing, the wafers were cleaned with acetone, isopropyl alcohol, and de-ionized water, and subsequently dehydrated in a convection oven at 120 °C for 20 min to maximize adhesion between the SiO_2 layer and the PR.

SU-8 2002 PR was used as carbon precursor for the planar IDEAs (MicroChem, Westborough, MA). Approximately 10 ml of PR were spin-coated on the silicon wafer to a thickness of 3 μm. A soft bake step was then carried out to evaporate solvent from the PR and the thin resist layer was ultraviolet (UV)-exposed through a photomask with the IDEA patterns. UV exposure triggers crosslinking of the exposed photoresist. A postexposure bake was then used to accelerate PR polymerization. Uncrosslinked PR was removed from the substrate by immersing the wafer in SU-8 developer (MicroChem).

A second photolithographic patterning was carried out on top of the planar structures to develop HAR microposts thus increasing the overall electrode surface area. For this, SU-8 2025 and 2050 were used to obtain PR layers of 80 μm and 160 μm, respectively. A mask aligner was used to line up the second photomask to the planar structures (MA56, Süss MicroTec, Garching, DE).

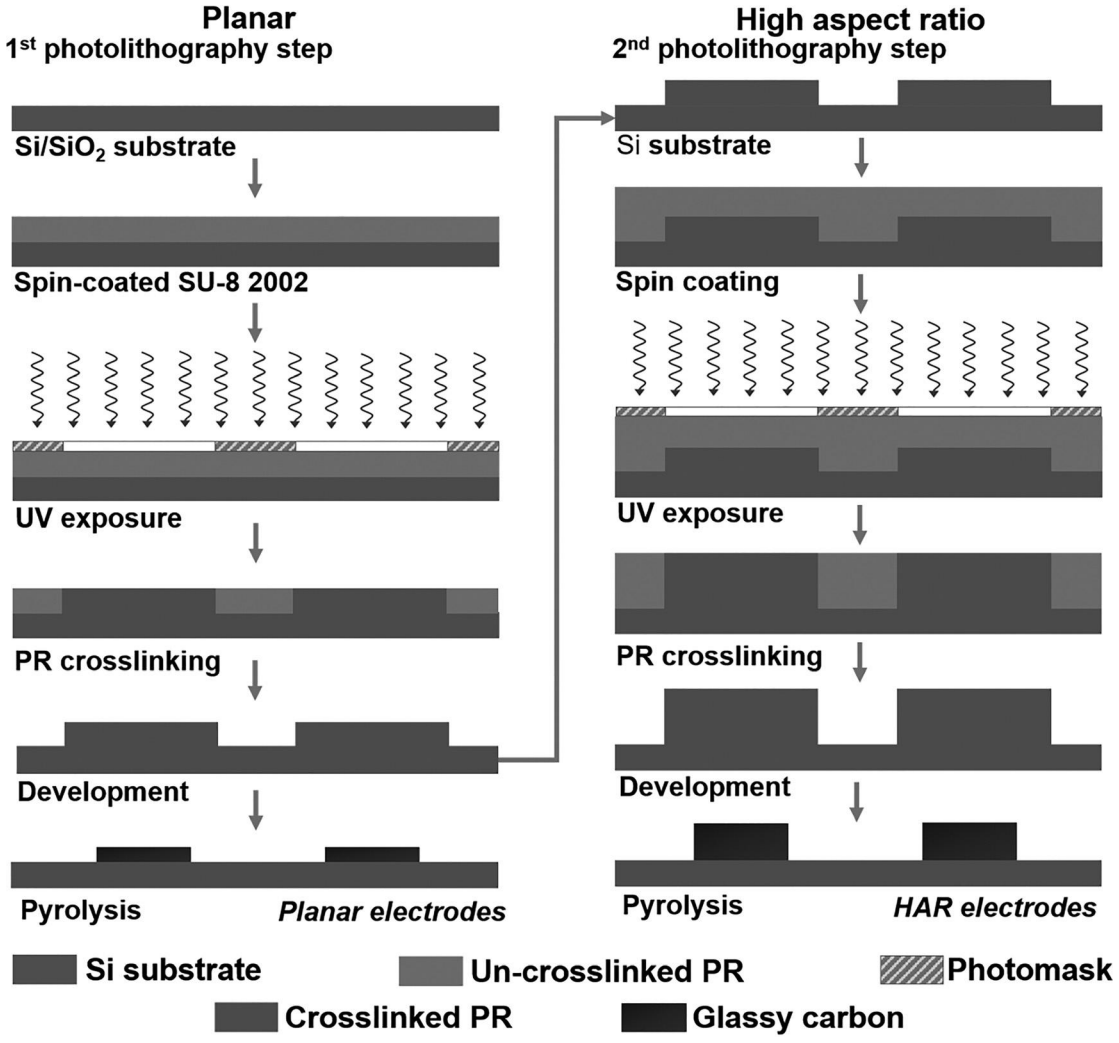

Fig. 3 Two-step carbon-MEMS fabrication process for the development of asymmetric coplanar electrodes (first photolithography step) and HAR microposts on top of planar structures (second photolithography step)

Table 1 Type of SU-8 PR and photolithography parameters for each microstructure: planar electrodes, and 80 μm and 160 μm-height microposts

SU-8 type	Spin-coating	Soft bake	UV exposure energy (mJ/cm^2)	Postexposure bake	Development time (min)
2002	1000 rpm for 30 s	2 min at 95 °C	90	2 min at 95 °C	1
2025	1000 rpm for 30 s	3 min at 65 °C and 9 min at 95 °C	215	2 min at 65 °C and 7 min at 95 °C	7
2050	1000 rpm for 30 s	7 min at 65 °C and 30 min at 95 °C	260	5 min at 65 °C and 12 min at 95 °C	15

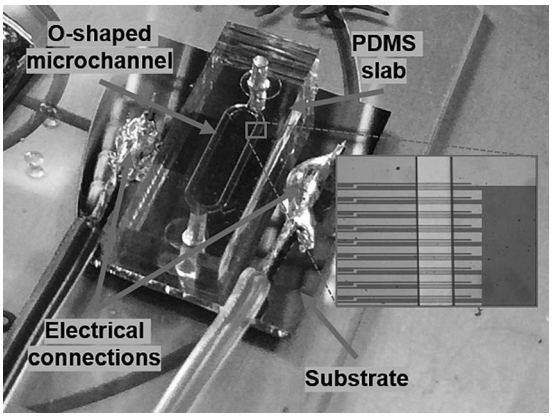

Fig. 4 Microfluidic chip containing AC electroosmotic pump; inset is showing the asymmetric electrodes that create micro-pump confined by the microchannel

Figure 3 depicts the complete fabrication process including patterning of coplanar (step 1) and HAR (step 2) microstructures. Table 1 includes process parameters used for the two discussed patterning steps.

The PR structures were then pyrolyzed in an open-ended tube furnace (Mini #40, R.D. Webb Company, Inc., Natick, MA) with N_2 gas flowing through at 2000 sccm. Pyrolysis was carried out in three steps: (a) temperature was increased from room temperature to 300 °C at a 5 °C/min ramp rate and kept at 300 °C for 1 h; (b) the temperature is increased from 300 °C to 900 °C at the same ramp rate and maintained at that maximum temperature for 1 h. Finally, (c) the furnace is turned off to passively cool down to room temperature. N_2 flow is suspended below 150 °C during cool down step.

2.2 Experimental Setup. For experimental testing, O-shaped microchannels were used to avoid pressure differentials and thus having the measured velocity change be attributed solely to electroosmotic flow [6]. The channels were patterned in PDMS slabs (Sylgard 184, Dow Corning Corp, Midland, MI) by soft-lithography. The patterned PDMS block was bonded to the silicon die after an air plasma treatment. The channels are 500 μm wide and 100 μm high. Copper wires were soldered to the IDEA pads and sealed with an epoxy resin. Figure 4 shows the fabricated device used in the study.

Experiments were carried out using a solution comprised of bidistilled water (on a conductivity of $\sigma = 1.72$ μS/cm) containing 1 μm-diameter latex microbeads as tracer particles. The electrodes were connected to a sinewave generator (33210 A, Agilent Technologies, Santa Clara, CA) and to an oscilloscope (TDS 2014B, Tektronix, Inc., Beaverton, OR) for signal monitoring. For each of the three electrode geometries, six different frequencies were tested: 1 kHz, 2 kHz, 10 kHz, 20 kHz, 100 kHz, and 200 kHz; and for each frequency, the signal amplitude was swept from 2 to 20 V_{PP}. Over 30 s video clips were recorded for each amplitude step to subsequently determine the fluid velocity using particle tracking software (ImageJ, National Institutes of Health, Bethesda, MD).

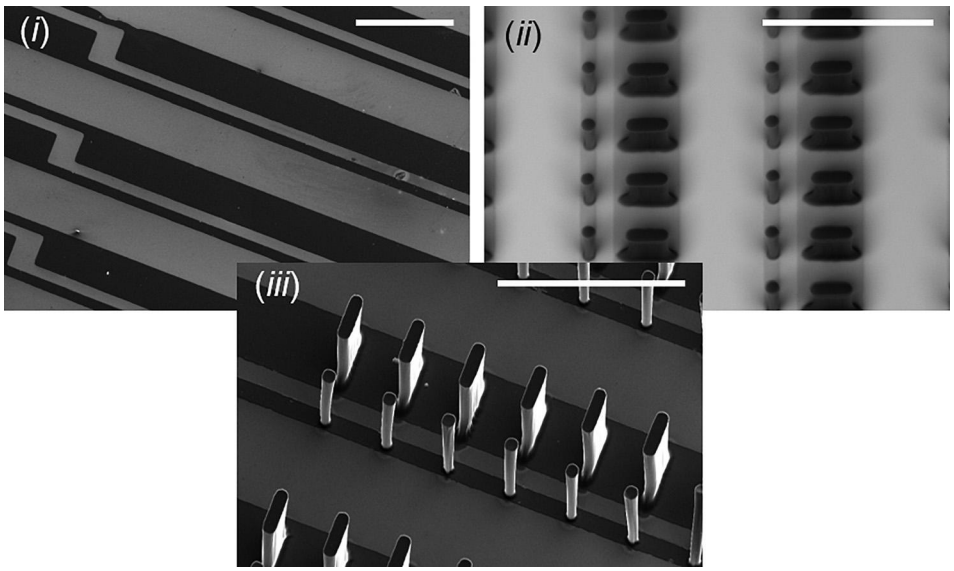

Fig. 5 Scanning-electron micrographs of the fabricated GC micro-electrodes: (*i*) asymmetric coplanar electrodes, (*ii*) asymmetric coplanar electrodes with 40 μm-height microposts, and (*iii*) asymmetric coplanar electrodes with 80 μm-height microposts. Scale bars = 200 μm.

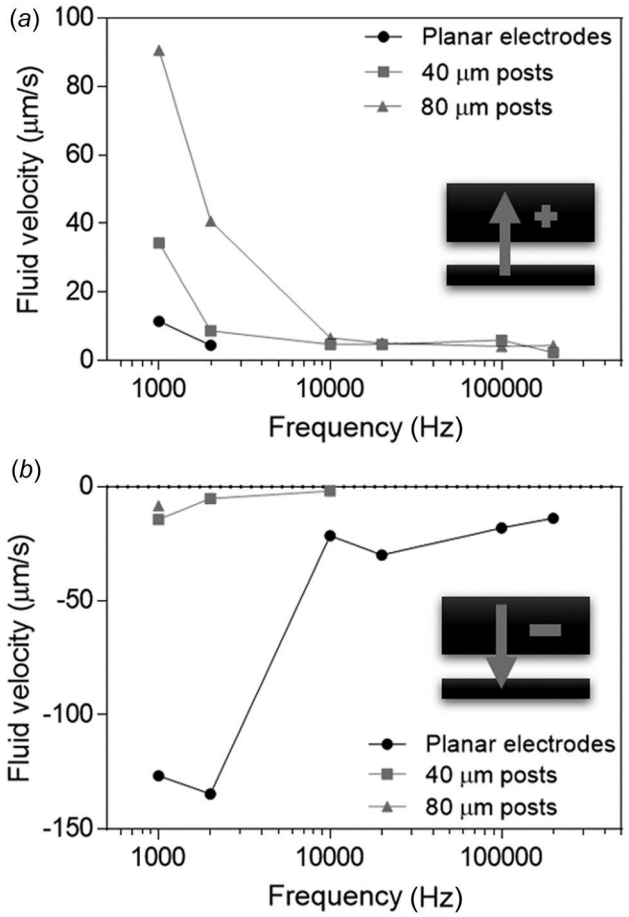

Fig. 6 Maximum (*a*) forward and (*b*) backward fluid velocities for frequency range from 1 to 200 kHz for planar electrodes, planar electrodes with 40 μm-height microposts and planar electrodes with 80 μm-height microposts

3 Results

After pyrolysis, the structures shrank approximately 50% in height due to the release of noncarbon elements from the PR molecules to the environment by the action of the high temperature. This shrinkage was verified via confocal microscopy, which showed an average height of 1.28 ± 0.07 μm, 37.75 ± 0.12 μm, and 72.62 ± 0.36 μm for pumps (*i*), (*ii*), and (*iii*), respectively. Figure 5 presents scanning electron microscopy (SEM) images of the three types of micro-electrodes.

Velocity test results show that asymmetric coplanar electrodes (i.e., device (*i*)) can develop forward net flow (from E_N to E_W) only at the lower frequencies (e.g., 1 and 2 kHz), while for higher frequencies, only reverse flow is developed. Figure 6 shows maximum fluid velocities in both, (*a*) forward and (*b*) backward directions achieved at different AC frequency conditions.

However, as can also be seen from Fig. 6, the presence of microposts atop of coplanar electrodes precludes the flow inversion, accompanied by the overall reduction in fluid flow (as compared to planar electrode structure). The most pronounced flow inversion is evident for planar electrodes where forward flow velocity is significantly lower than the backflow that takes place after flow inversion. For 40 μm-height posts-containing electrodes, a low-magnitude backward flow is observed only at the lowest frequencies (1, 2, and 10 kHz in Fig. 6(*b*)), whereas a significant forward flow is observed for these electrodes in the entire range of frequencies tested (from 1 to 200 kHz in Fig. 6(*a*)).

The effect of microposts becomes more evident for the 80 μm-height posts electrodes, where forward flow at low frequencies achieves much greater velocity than planar or 40 μm-height post electrodes, while the backflow is developed only at 1 kHz.

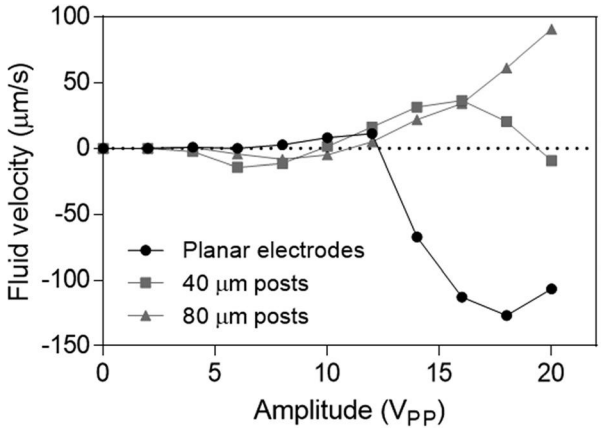

Fig. 7 Fluid velocity development with respect to the AC amplitude sweep at 1 kHz for planar electrodes, planar electrodes with 40 μm-height microposts and planar electrodes with 80 μm-height microposts

Flow direction reversal presumably occurs due to the increased size of the dominating vortex formed above the wide electrode. For micropost electrodes, small distance is left between the tops of postelectrodes and microfluidic channel's ceiling. Thus, complex vortex (over the wide electrode)–vortex (over the narrow electrode) interaction as well as redirection of the fluid streamlines by the channel ceiling combine to create flow patterns and backflow conditions that depend strongly on electrodes' and channel's geometry. We believe that this effect possibly occurs due to vortices that form along the height of adjacent microposts suppressing rise of the vortices generated at the surface of planar structures to reach the microchannel ceiling, thus avoiding flow reversal.

The highest fluid velocities for all three devices were achieved at 1 kHz. Early tests of the microposts showed that higher velocities can possibly be reached at even lower frequencies (e.g., 100 and 200 Hz) however, as the AC amplitude increases above 10 V_{PP}, electrolysis occurs, leading to electrode destruction. Also, at frequencies higher than 200 kHz, no EDL induction was noticed, possibly due to the extremely high-electrode polarization switching preventing suspended counter-ions to reach the electrode surface.

Figure 7 shows fluid velocity development at 1 kHz with respect to the AC amplitude sweep from 2 to 20 V_{PP}. Here, the higher-fluid velocities are achieved at the higher-AC amplitudes (i.e., 8–20 V_{PP}). For the specific case of device (*i*), this corresponds to the formation of larger dominant vortices, accordingly to the higher-magnitude applied electric field. For post electrodes, it is likely that vortices that develop along the vertical surface of the posts might interfere with other vortices that form at the planar section of the electrodes, preventing flow direction reversal. It is notable that at the highest AC amplitudes, fluid velocities between devices (*i*) and (*iii*) become comparable in magnitude, possibly meaning that without the action of the planar electrodes' surface, micropost would develop even higher-fluid velocities in the forward direction.

4 Conclusions

The carbon-MEMS fabrication process allows for the efficient fabrication of glassy carbon high-surface area structures which otherwise are difficult and/or expensive to make with other materials and fabrication processes. In this study, we demonstrated that asymmetric coplanar electrodes develop the higher-fluid velocities when contrasted to high-surface-area structures. However, the implementation of microposts as vertical extensions of planar electrodes, while leading to some fluid velocity decrease, may be useful in situations where flow reversal is not wanted.

Furthermore, we believe that the optimization of the micropost separation developed along the surface of the planar structures would lead to comparable velocities in both forward and backward directions. This has a great potential in applications where tunable back and forth pumping is required. Microposts can also be used as blockage structure for microfluidic mixing, commonly difficult to achieve at small Reynolds numbers characteristic of the flow in microchannels.

Funding Data

- UC-Mexus-CONACyT Collaborative Grant (UCM-104728; Funder IDs: 10.13039/100005909, 10.13039/501100003141).
- UC-Mexus Small Grant (UCM-104199; Funder IDs: 10.13039/100005909, 10.13039/501100003141).
- CONACyT National Scholarship Program (#322105; Funder IDs: 10.13039/100005909, 10.13039/501100003141).
- National Science Foundation (Award CMMI-100000147; Funder ID: 10.13039/100000001).

References

[1] Madou, M. J., Lal, A., Schmidt, G., Song, X., Kinoshita, K., Fendorf, M., Zettl, A., and White, R., 1997, "Carbon Micromachining (C-MEMS)," Electrochem. Soc. S, **97**, pp. 61–69.

[2] Martinez-Duarte, R., Renaud, P., and Madou, M. J., 2011, "A Novel Approach to Dielectrophoresis Using Carbon Electrodes," Electrophoresis, **32**(17), pp. 2385–2392.

[3] Vazquez-Pinon, M., Benítez, B. C., Pramanick, B., Perez-Gonzalez, V. H., Madou, M. J., Martinez-Chapa, S. O., and Hwang, H., 2017, "Direct Current-Induced Breakdown to Enhance Reproducibility and Performance of Carbon-Based Interdigitated Electrode Arrays for AC Electroosmotic Micropumps," Sens. Actuators A: Phys., **262**, pp. 10–17.

[4] Islam, N., and Reyna, J., 2012, "Bi-Directional Flow Induced by an AC Electro-osmotic Micropump With DC Voltage Bias," Electrophoresis, **33**(7), pp. 1191–1197.

[5] Liu, W., Shao, J., Ren, Y., Wu, Y., Wang, C., Ding, H., Jiang, H., and Ding, Y., 2016, "Effects of Discrete-Electrode Arrangement on Traveling-Wave Electroosmotic Pumping," J. Micromech. Microeng., **26**(9), p. 095003.

[6] Studer, V., Pépin, A., Chen, Y., and Ajdari, A., 2004, "An Integrated AC Electrokinetic Pump in a Microfluidic Loop for Fast and Tunable Flow Control," Analyst, **129**(10), pp. 944–949.

[7] Garcia-Sanchez, P., Ramos, A., Green, N. G., and Morgan, H., 2006, "Experiments on AC Electrokinetic Pumping of Liquids Using Arrays of Microelectrodes," IEEE Trans. Dielectr. Electr. Insul., **13**(3), pp. 670–677.